Detection of signs of Parkinson's disease using dynamical features via an indirect pointing device

Rosane Ushirobira, Denis Efimov, Géry Casiez, Laure Fernandez, Fredrik Olsson, Alexander Medvedev

HAL Id: hal-02887913

https://inria.hal.science/hal-02887913

Submitted on 2 Jul 2020

Detection of signs of Parkinson's disease using dynamical features via an indirect pointing device ⋆

Rosane Ushirobira * **Denis Efimov** * **Géry Casiez** ** **Laure Fernandez** ***
Fredrik Olsson **** **Alexander Medvedev** ****

** Inria, Univ. Lille, CNRS, UMR 9189 – CRIStAL, F-59000 Lille, France.
(e-mail: {Rosane.Ushirobira, Denis.Efimov}@inria.fr)*
*** Univ. Lille, Inria, CNRS, UMR 9189 – CRIStAL, F-59000 Lille, France,
Institut Universitaire de France (IUF) (e-mail: Gery.Casiez@univ-lille.fr)*
**** Aix-Marseille Université, CNRS, ISM, Marseille, France (e-mail:
Laure.Fernandez@univ-amu.fr)*
***** Information Technology, Uppsala University, Box 337, Uppsala SE-751
05, Sweden (e-mail: {Fredrik.Olsson, Alexander.Medvedev}@it.uu.se)*

Abstract: In this paper, we study the problem of detecting early signs of Parkinson's disease during an indirect human-computer interaction via a computer mouse activated by a user. The experimental setup provides a signal determined by the screen pointer position. An appropriate choice of segments in the cursor position raw data provides a filtered signal from which a number of quantifiable criteria can be obtained. These dynamical features are derived based on control theory methods. Thanks to these indicators, a subsequent analysis allows the detection of users with tremor. Real-life data from patients with Parkinson's and healthy controls are used to illustrate our detection method.

Keywords: Quantification of physiological parameters for diagnosis and treatment assessment. Developments in measurement, signal processing. Control of physiological and clinical variables.

1. INTRODUCTION

Parkinson's disease (PD) is accounted for affecting currently between seven to ten million people in the world (Pahwa et al., 2020). This is the second most common neuro-degenerative illness, that is age-related, right after Alzheimer's disease. The cardinal motor symptoms of PD include rigidity, bradykinesia, rest tremor, and postural instability (Louis et al., 2015). The motor symptoms result from the degeneration and loss of dopaminergic neurons in the substantia nigra of the basal ganglia and, consequently, dopamine deficiency. It can take four to six years for the disease onset with PD motor problems becoming noticeable (Alves et al., 2008). For the time being, there is no cure for this illness, but an appropriate treatment can strongly improve the symptoms, especially at its beginning.

More than 1.2 million people in Europe live with PD and the annual cost for patients, caregivers, and healthcare was in 2011 estimated to €13.9 billion (European Parkinson's Disease association, 2014). The number of people with Parkinson's is expected to double by 2030 (Dorsey et al., 2007). Early treatment of PD can potentially reduce its economical impact, improve life quality of patients and, probably, delay the progression of the disease. However, the matter of medication treatment in early PD is currently under debate (Stocchi et al., 2015). Traditionally, it is recommended to delay medication until the motor symptoms of PD start influencing the patient's quality of life. This point of view is based on the fact that anti-Parkinsonian drugs (*e.g.* Levodopa) induce side effects and lose efficacy with time. An alternative hypothesis to consider is that medication at early stages of PD might support restoration of the impacted brain structures and delay the irreversible loss of function (Schapira and Obeso, 2006). Thus an early and better diagnostics would be desirable for an efficient treatment.

While Parkinsonian patients may not experience certain disease symptoms at all, others' symptoms are likely to fluctuate and vary from day to day (Politis et al., 2010). Tremor is one of the cardinal motor symptoms linked to PD, causing involuntary oscillatory motion in extremities, in particular in the hands. It can severely limit a person's ability to use computers. However, tremor is not always present in early (and even in advanced) stages of PD (Davie, 2008). Furthermore, even a healthy person can experience prominent physiological tremor due to fatigue, stress or as symptom of withdrawal of drugs or alcohol. So, tremor is not specific to PD and also appears in other diseases and conditions. Moreover, other PD symptoms may be present, such as limb stiffness (Koller and Montgomery, 1997), often causing movements to be slow and cramped. In contrast, hand tremor can result in a movement of a relatively high velocity.

There exist research works in dealing with different aspects of PD through control-theoretical approaches. A very thorough survey, though not so recent, on control theory perspective in the study of PD can be found in Schiff (2010). The matter of oscillation in neural structures has drawn significant attention, see *e.g.* García et al. (2013), Davidson et al. (2012). Also, from a clinically oriented perspective, symptoms quantification and therapy individualization/optimization are addressed. For instance, in Jansson et al. (2015), two anomaly detection methods were proposed to distinguish between PD patients and healthy control subjects, based on eye-tracking data. In

addition, to quantify the severity of tremor in PD patients undergoing deep brain stimulation (DBS), Olsson and Medvedev (2018) used Markov chains on the data from the inertial measurement units. In Haddock et al. (2017), the authors proposed a model-predictive control strategy for closed-loop DBS. An optimization-based approach to the individualization of DBS is described in Medvedev et al. (2019).

PD is usually evaluated through a score obtained in clinics. The current standard to evaluate motor signs is the Unified Parkinson's Disease Rating Scale Part III (UPDRS-III) (Martínez-Martín et al., 1994). This method requires trained clinicians and each such measurement can only be done once or at best twice a year. The procedure takes hours and demands patient cooperation. Due to several factors, large symptomatic variability is observed through this score and the daily life of patients at home. This variability clearly demonstrates the relevance of an ecological study making use of a non-obtrusive data collection technology. As a matter of fact, a non-obstructive symptom registration and quantification can also be useful in monitoring the therapeutic effect and optimizing medical treatment of PD.

Within a human-computer interaction (HCI) framework, a recent study shows that most patients use a laptop or desktop computer and keep using a computer mouse and keyboard instead of looking for alternative solutions (Hartikainen and Ovaska, 2015). These input devices can be used to collect and analyze motor data from users. For example, Giancardo et al. (2016) discovered patterns in the time series of key hold times. Using an ensemble regression algorithm, they discriminated PD from control participants with an AUC[1] of 0.81. White et al. (2018) first suggested that mouse movements can be used to distinguish people with PD from others. They used mouse cursor position from a search engine, from around a total of 800 users and investigated the use of a number of features to detect PD. However the internal validity of their results is limited since participants searching for terms on PD symptoms were considered as affected.

Control theoretical methods are not yet commonly used in HCI problems (see an interesting survey in Oulasvirta (2018)). A relevant work can be found in Aranovskiy et al. (2019) where the first dynamic model was designed to describe a fundamental task in HCI, the pointing task, that can be described simply as reaching a target with a cursor from an initial position, for instance when the user executes a movement to select a particular icon on the screen.

The goal of the present paper is to use control theory methods on the detection of tremor of PD patients within a HCI framework.

The exposition includes the following steps. In Section 2, the experimental setup is described, notably on data collected and the position signal processing. The quantifiable dynamical features are explained in Section 3. Real-life data are then analyzed accordingly to the features and the result is given in Section 4.

2. EXPERIMENTAL SETUP

In the experiment, the participants installed on their computers an application running in background to record mouse pointer

---

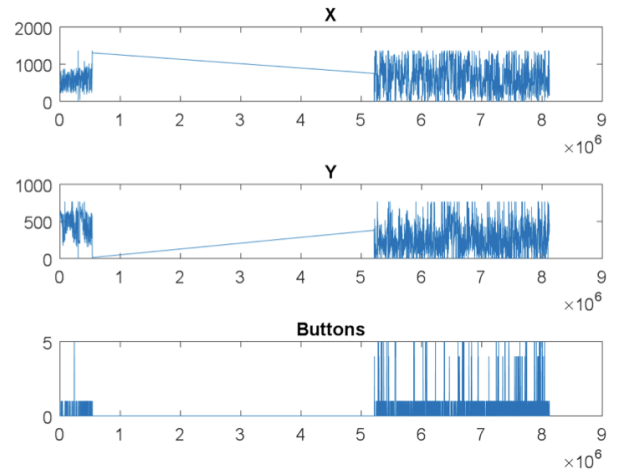[1] AUC stands for Area Under The Curve ROC (Receiver Operating Characteristics) curve

Fig. 1. A sample of a user's movements in the x and y coordinates and the click buttons (pixels versus time in ms)

coordinates on screen and the state of mouse buttons while they normally used their computers. The collected information was recorded in a SQLite file and sent to a remote server on a daily basis. The application was written in C++ and used libpointing (Casiez and Roussel, 2011) to get the screen physical dimensions. In this way, mouse coordinates may be converted from pixels to physical units (*e.g.* mm), to normalize different screen resolutions and pixel densities. After installation, the participants filled an online questionnaire to collect demographic and medical data (degree of severity of Parkinson's disease). All data were collected anonymously. Fig. 1 shows a sample of a user's movements in the *x* and *y* coordinates, together with the click buttons.

All computer mouse movements are relevant in the study of the user behavior. Nevertheless, a systemic analysis must involve explicit characteristics allowing the quantification of the phenomena. To determine distinguished features in the movement, our first step was to focus on the movement sections corresponding to specific tasks.

The behavior of the mouse pointer on the computer screen while the user is performing some tasks can be certainly influenced by his/her physical/mental state (see for instance Pimenta et al. (2013)). The pointing task is one of the most executed interactions between the user and the computer. Considering our previous work providing a dynamical model of pointing tasks (Aranovskiy et al., 2019), we chose to segment the original data to accentuate the pointing tasks done by the user. The result is shown in Fig. 2.

The end of a pointing task is characterized by a mouse button click. The fact of choosing pointing tasks is reinforced by the presence of particular symptoms in PD patients such as tremor and oscillating behavior, as well decreasing movement speed (Fernandez et al., 2018), which can also be more easily observed during pointing.

Pointing tasks can be split into two distinctive phases: a ballistic phase with no visual feedback processing, where the user rapidly brings the pointer close to the target, and a tracking phase accompanied by a visual feedback, where the user finishes the task by a mouse click in this study. Two examples of mouse position signal during pointing are illustrated in Fig. 3.
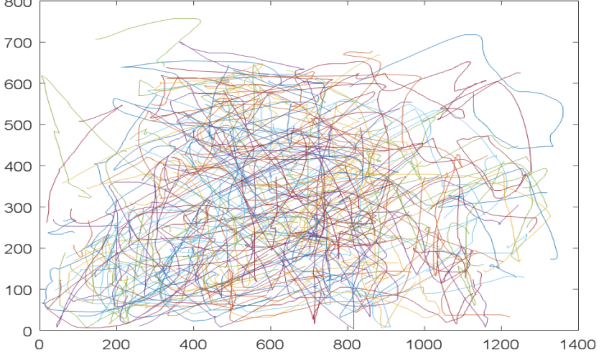
Fig. 2. A sample of pointing tasks in a user's movements, each pointing task is distinguished by different colors, the axes represent pixels in the y and x coordinates
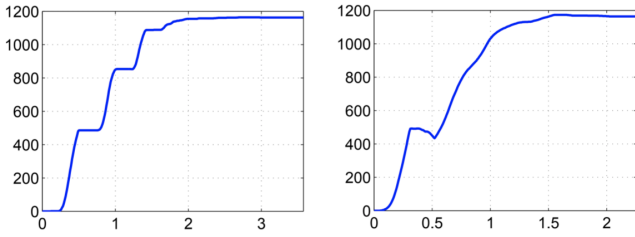

Fig. 3. Examples of mouse position signal in pointing tasks, the axes indicate the cursor position in pixels versus time in seconds

Having segmented pointing motions for each user, several quantifiers were proposed to analyze the data (for instance, concerning the velocity and the oscillations movements). These dynamical features are described in the next section.

3. DYNAMICAL FEATURES

As mentioned in the previous section, the data are separated into recognizable signals to guarantee relevant quantification. Hence, after a preliminary processing, the measured data are decomposed in $n > 0$ segments of pointing motions (n may be different for each user) containing the following information: for $i = 1, \ldots, n$ and $k = 1, \ldots, N_i$ where $N_i > 0$ is the size of the segment dataset,

- $x_{i,k}$, $y_{i,k}$ represent the position of the pointer,
- $t_{i,k}$ corresponds to the time stamp.

It is assumed that $x_{i,1}$, $y_{i,1}$ is the position of the beginning of the pointing at time $t_{i,1}$, and that in x_{i,N_i}, y_{i,N_i} at instant t_{i,N_i} a button click is activated, for all $i = 1, \ldots, n$.

For all $k = 1, \ldots, N_i$ and $i = 1, \ldots, n$, we define the following auxiliary variables calculated for each segment:

- $\dot{x}_{i,k}$, $\dot{y}_{i,k}$ estimate the pointer velocity,
- $\ddot{x}_{i,k}$, $\ddot{y}_{i,k}$ estimate the pointer acceleration,
- $\dot{x}^a_{i,k}$, $\dot{y}^a_{i,k}$ are the averaged velocity of the pointer derived as

$$\dot{x}^a_{i,k} = \frac{\xi_{i,k} - \xi_{i,k-N_i}}{t_{i,k} - t_{i,k-N_i}}, \ \dot{y}^a_{i,k} = \frac{\psi_{i,k} - \psi_{i,k-N_i}}{t_{i,k} - t_{i,k-N_i}},$$

where $\xi_{i,k} = \xi_{i,k-1} + (t_{i,k} - t_{i,k-1})\dot{x}_{i,k}$ with $\xi_{i,0} = 0$ and $\psi_{i,k} = \psi_{i,k-1} + (t_{i,k} - t_{i,k-1})\dot{y}_{i,k}$ with $\psi_{i,0} = 0$.

In order to calculate the estimates $\dot{x}_{i,k}$, $\dot{y}_{i,k}$, $\ddot{x}_{i,k}$ and $\ddot{y}_{i,k}$ a homogeneous differentiator has been used, whose description

can be found in Nancel et al. (2018). This nonlinear filter was applied to the whole dataset before its segmentation and extraction of the pointing motions.

In the following, the proposed dynamical features are defined for each pointing segment $i = 1, \ldots, n$ using the data introduced above. Some of these features, such as the ones given in the next subsection, are mere quantifiers of the measured signals and their derivatives, but others are directly oriented to the detection of presence of parasitic oscillations, when the fault detection and isolation theory is indirectly applied (Isermann, 1997).

3.1 Average of absolute values of velocities and accelerations

This feature computes the absolute values $\bar{\bar{x}}_i$, $\bar{\bar{y}}_i$, $\bar{\bar{x}}_i$ and $\bar{\bar{y}}_i$ of velocities $\dot{x}_{i,k}$, $\dot{y}_{i,k}$ and accelerations $\ddot{x}_{i,k}$, $\ddot{y}_{i,k}$, respectively:

$$\bar{x}_i = \frac{1}{N_i} \sum_{k=1}^{N_i} |\dot{x}_{i,k}|, \ \bar{y}_i = \frac{1}{N_i} \sum_{k=1}^{N_i} |\dot{y}_{i,k}|,$$

$$\bar{\bar{x}}_i = \frac{1}{N_i} \sum_{k=1}^{N_i} |\ddot{x}_{i,k}|, \ \bar{\bar{y}}_i = \frac{1}{N_i} \sum_{k=1}^{N_i} |\ddot{y}_{i,k}|.$$

Roughly speaking it corresponds to the velocity and acceleration energies (accumulated power of a user).

3.2 Velocity oscillation

This feature quantifies the number of sign changes of the velocities $\dot{x}_{i,k}$, $\dot{y}_{i,k}$ during the slow phase of the pointing task (see Subsection 3.6). Denote these numbers as $n_i^{\dot{x}}$ and $n_i^{\dot{y}}$, then the following expressions are proposed:

$$n_i^{\dot{x}} = n_i^{\dot{x}} + 1 \text{ if } \dot{x}_{i,k}\dot{x}_{i,k-1} < 0 \text{ and } |\dot{x}_{i,k}| < v_i^{\dot{x}},$$
$$n_i^{\dot{y}} = n_i^{\dot{y}} + 1 \text{ if } \dot{y}_{i,k}\dot{y}_{i,k-1} < 0 \text{ and } |\dot{y}_{i,k}| < v_i^{\dot{y}}, \ k = 1, \ldots, N_i,$$

where
$$v_i^{\dot{x}} = \kappa \max_{k=1,\ldots,N_i} |\dot{x}_{i,k}|, \ v_i^{\dot{y}} = \kappa \max_{k=1,\ldots,N_i} |\dot{y}_{i,k}|$$

correspond to the maximal velocities, and $\kappa \in (0,1)$ is a tuning parameter that determines the rate level in the slow phase of the motion (we used $\kappa = 0.2$ in the experiments). For computation of these features, the averaged velocities $\dot{x}^a_{i,k}$, $\dot{y}^a_{i,k}$ can be used (to avoid the dependence of the criterion on the measurement noises), while the condition on smallness of the velocities can be omitted.

3.3 Pointing error increments

The pointing motion is usually stable (for experienced users, see Aranovskiy et al. (2019)) and the errors of pointing $E^x_{i,k}$ and $E^y_{i,k}$, which can be defined as the differences with respect to the final position:

$$E^x_{i,k} = x_{i,k} - x_{i,N_i}, \ E^y_{i,k} = y_{i,k} - y_{i,N_i},$$

for $k = 1, \ldots, N_i$ and $i = 1, \ldots, n$, are monotonously decreasing. Any increments in $E^x_{i,k}$ and $E^y_{i,k}$ can be considered as a user mistake, which would likely increase in quantity as PD symptoms grow more severe. Hence, the amount of the pointing error increments e^x_i and e^y_i in the (final) slow phase of the motion can be calculated as follows:

$$e^x_i = e^x_i + 1 \text{ if } \dot{x}_{i,k}E^x_{i,k} > 0, \ k = K_x, \ldots, N_i,$$
$$e^y_i = e^y_i + 1 \text{ if } \dot{y}_{i,k}E^y_{i,k} > 0, \ k = K_y, \ldots, N_i,$$

$$K_x = \arg \inf_{k=K_x,\ldots,N_i} |\dot{x}_{i,k}| \le v_i^{\dot{x}}, \ K_y = \arg \inf_{k=K_y,\ldots,N_i} |\dot{y}_{i,k}| \le v_i^{\dot{y}},$$

The idea of these features can be interpreted as follows. We can assume that the pointing motion is stable with a simple quadratic Lyapunov function $V_x(E^x_{i,k}) = (E^x_{i,k})^2$ or $V_y(E^y_{i,k}) = (E^y_{i,k})^2$, then the instability conditions $\dot{V}_x(E^x_{i,k}) > 0$ or $\dot{V}_y(E^y_{i,k}) > 0$ correspond to $\dot{x}_{i,k}E^x_{i,k} > 0$ or $\dot{y}_{i,k}E^y_{i,k} > 0$, respectively, which is used to calculate e^x_i and e^y_i. In such a case, e^x_i and e^y_i evaluate the time interval of "instability" for the pointing motion. Of course, a more complex Lyapunov function with cross terms (in 2D) can also be tested.

3.4 Mean error

Another way to estimate the pointing motion "instability" consists in acquiring the average value of the Lyapunov function during the slow phase of the motion. Note that in our case, we have always $E^x_{i,N_i} = E^y_{i,N_i} = 0$ by construction (the desired point is reached and the pointing dynamics is converging). Consequently, if the errors $E^x_{i,k}$ and $E^y_{i,k}$ stay big in average during the visual phase, then the motion admitted a perturbation (oscillations or tremor issued by decease, for instance). Hence, we can compute the mean errors ε^x_i and ε^y_i in the final slow phase of the pointing task:

$$\varepsilon^x_i = \frac{1}{N_i - K_x} \sum_{k=K_x}^{N_i} |E^x_{i,k}|, \quad \varepsilon^y_i = \frac{1}{N_i - K_y} \sum_{k=K_y}^{N_i} |E^y_{i,k}|.$$

For healthy users, these errors originate from unperturbed stable dynamics and have to be smaller.

3.5 Physiological features

There are conventional parameters usually applied in the HCI community to quantify any pointing motion: the time before click, the average speed of pointing and percentage of pointing motion (Soukoreff and MacKenzie, 2004).

The time before click T_i corresponds to the generic reaction of a user: how much time is needed for him/her to activate a button once the goal position is reached by the mouse pointer. An additional lag can be present in the case of a disease. Since the data are generated on an event-based acquisition in the system, if the mouse is not moved or not activated, then there is no measurement triple $(t_{i,k}, x_{i,k}\, y_{i,k})$, and the time T_i before click is just the difference between the time stamps at the end:

$$T_i = t_{i,N_i} - t_{i,N_i-1}.$$

The average speed a_i of the pointing motion is calculated in 2D:

$$a_i = \frac{\sqrt{\left(E^x_{i,1}\right)^2 + \left(E^y_{i,1}\right)^2}}{t_{i,N_i} - t_{i,1}},$$

and it does not take into account the curvature of the trajectory.

The last feature in this subsection is the percentage $\delta\tau_i$ of pointing motion after the maximal speed:

$$\delta\tau_i = \frac{\tau_i}{N_i} \text{ where } \tau_i = \arg \sup_{k=1,\ldots,N_i} w_{i,k} = w_{i,\max}$$

with $w_{i,k} = \sqrt{\dot{x}^2_{i,k} + \dot{y}^2_{i,k}}$, $k = 1,\ldots,N_i$ and $w_{i,\max} = \max_{k=1,\ldots,N_i} w_{i,k}$.

The instant of the maximal velocity can be related with the first stage of the ballistic motion, then the time of the pointing task passed after the maximal velocity is related with the visual corrective movement, whose length is usually augmented in the case of PD users.
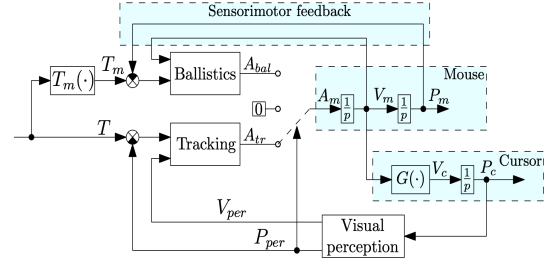

Fig. 4. The dynamical pointing model structure (Aranovskiy et al., 2019)

3.6 Pointing model

A dynamical model of the pointing motion was proposed in Aranovskiy et al. (2019), whose identified parameters are applied as a feature here. The model Aranovskiy et al. (2019) is a switched dynamic system, which characterizes the cursor movements in indirect pointing tasks (*e.g.*, using the computer mouse for pointing). As in Müller et al. (2017), there are two distinct phases involved in the model: a ballistic movement phase realized by a nonlinear model in Lurie form and a corrective movement phase governed by a visual feedback linear system. The switched nature of the model is originated by commutation between these phases. The block scheme given in Fig. 4 provides the pointing model structure. In this figure, T_m is the desired mouse position (estimated by the user under the reference value T), A_m denotes the acceleration, V_m is the velocity and P_m is the position of the mouse, G is the pointing transfer function (usually just a linear static or a sigmoid function), V_c and P_c are the velocity and the position of the cursor, V_{per} and P_{per} are the perceived velocity and position of the cursor. Depending whether the pointing task is in the ballistic phase or in the tracking phase, that makes the switch of A_m from A_{bal}, 0 (not an immediate switch) or A_{tr}. Following the details given in Aranovskiy et al. (2019), for a linear function G, the model in the final corrective phase can be reduced to a second order dynamics:

$$\theta^x_2 \ddot{x}_{i,k} + \theta^x_1 \dot{x}_{i,k} + x_{i,k} = x_{i,N_i}, \ \theta^y_2 \ddot{y}_{i,k} + \theta^y_1 \dot{y}_{i,k} + y_{i,k} = y_{i,N_i}$$

for all $k = K,\ldots,N_i$ and $i = 1,\ldots,n$, where $K = \min\{K_x, K_y\}$, $\theta^x_2 > 0$, $\theta^x_1 > 0$, $\theta^y_2 > 0$ and $\theta^y_1 > 0$ are the model parameters. It is easy to see that for any positive values of these parameters, $x_{i,k}$ approaches asymptotically x_{i,N_i}. In the presence of PD and related tremor, the model may loose its stability and the identified values of θ^x_2, θ^x_1, θ^y_2 and θ^y_1 can change the sign, which is used here for detection of the disease presence. Applying the least square approach, the estimates $\hat{\theta}^x_2$, $\hat{\theta}^x_1$, $\hat{\theta}^y_2$ and $\hat{\theta}^y_1$ of these parameters can then be used as features.

3.7 Estimation of amplitude of oscillations

The tremor of PD patients usually appears in the slow final phase of the motion, which can be approximately modeled as follows:

$$x_{i,k} = x_f + a_x \sin(\omega t_{i,k} + \phi_x) + v^x_{i,k},$$
$$y_{i,k} = y_f + a_y \sin(\omega t_{i,k} + \phi_y) + v^y_{i,k},$$

for $k = K,\ldots,N_i$ and $i = 1,\ldots,n$, where x_f and y_f are the constant (or quasi-constant, slowly varying in time) final states in x and y (they converge or are equal to x_{i,N_i} and y_{i,N_i}); ω is the tremor frequency, a_x, a_y and ϕ_x, ϕ_y are the amplitudes

and the phases of tremor oscillations, respectively; $v_{i,k}^x$ and $v_{i,k}^y$ are bounded functions of time, which correspond to the model errors, noises and uncertainties. The frequency is different depending on type of tremor. Most common for Parkinsonian tremor is rest tremor around 4 to 6 Hz, but can also contain postural tremor and action tremor up to 12 Hz, although this appears to be more rare (Deuschl et al., 2001). So ω can be assumed to be known, and one of these values can be used. The other quantities, *e.g.*, x_f, a_x and ϕ_x for $x_{i,k}$, can be taken as uncertain constants and estimated online. In such a case, the oscillation amplitudes a_x and a_y can be used for detection of the disease presence. Let us explain, considering $x_{i,k}$ only, how we can perform such an evaluation. To this end note that

$$x_{i,k} = x_f + a_x \sin(\omega t_{i,k})\sin(\phi_x) + a_x \cos(\omega t_{i,k})\cos(\phi_x) + v_{i,k}^x$$
$$= \theta_x^\top \eta_{i,k}^x + v_{i,k}^x,$$

where

$$\theta_x = \begin{bmatrix} x_f \\ a_x \sin(\phi_x) \\ a_x \cos(\phi_x) \end{bmatrix}$$

represents the vector of unknown parameters, and

$$\eta_{i,k}^x = \begin{bmatrix} 1 \\ \sin(\omega t_{i,k}) \\ \cos(\omega t_{i,k}) \end{bmatrix}$$

is the known regressor function, so the initial model is represented in the form of a linear regression. There is a large number of methods providing the estimation $\hat{\theta}_{i,k}^x$ of parameters θ_x in such a scenario, and the simplest gradient algorithm is a solution (Sastry and Bodson, 1989):

$$\hat{\theta}_{i,k+1}^x = \hat{\theta}_{i,k}^x + \gamma_x \eta_{i,k}^x \left(x_{i,k} - \eta_{i,k}^x (\hat{\theta}_{i,k}^x)^\top \right), \quad \hat{\theta}_{i,K}^x = 0,$$

where $\gamma_x > 0$ is a tuning parameter. A drawback of this algorithm is that it is impossible to accelerate the estimation error convergence (Efimov and Fradkov, 2015). An approach to overcome this shortage is to use the DREM method (Aranovskiy et al., 2017) to decouple the estimation processes, and also to use fixed-time estimators (Wang et al., 2019):

$$\hat{\theta}_{i,k+1}^x = \hat{\theta}_{i,k}^x + \eta_{i,k}^x (\gamma_{x+} \left[x_{i,k} - \eta_{i,k}^x (\hat{\theta}_{i,k}^x)^\top \right]^{1+\alpha_x}$$
$$+ \gamma_{x-} \left[x_{i,k} - \eta_{i,k}^x (\hat{\theta}_{i,k}^x)^\top \right]^{1-\alpha_x}), \hat{\theta}_{i,K}^x = 0,$$

where $\gamma_{x+}, \gamma_{x-} > 0$ and $\alpha_x \in [0,1)$ are tuning parameters. Then the average estimate of the amplitude of oscillations can be computed as follows:

$$a_i = \sum_{k=K}^{N_i} \sqrt{\left(\hat{\theta}_{i,k}^x \right)_2^2 + \left(\hat{\theta}_{i,k}^x \right)_3^2},$$

where $\left(\hat{\theta}_{i,k}^x \right)_2$ and $\left(\hat{\theta}_{i,k}^x \right)_3$ are the second and the third components of the vector $\hat{\theta}_{i,k}^x$ (by construction, $a_x = \sqrt{(\theta_x)_2^2 + (\theta_x)_3^2}$).

Remark 1. It is interesting to notice that some of the aforementioned features appear also in White et al. (2018), they are all of type *motor* and not model-based as in Subsections 3.6 and 3.7. In that work, a table with 57 features from a web search signal is presented, ordered according to their weight in their learner classifier. Many of the quantifiers are characterized by the specific experiment (involving queries, and so on). Some of their motor features are similar to ours, namely Minimum Cursor Y Coordinate with weight 0.247770 and rank 14, AVG acceleration of mouse cursor (0.239814, 16), AVG velocity of
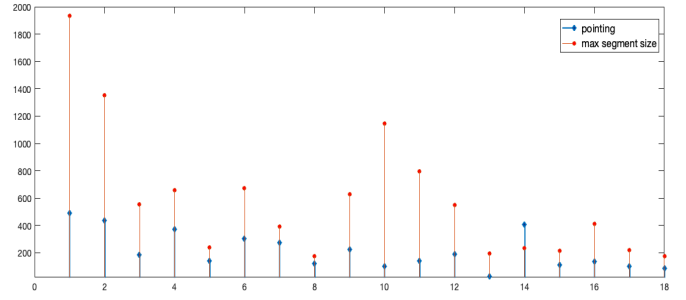

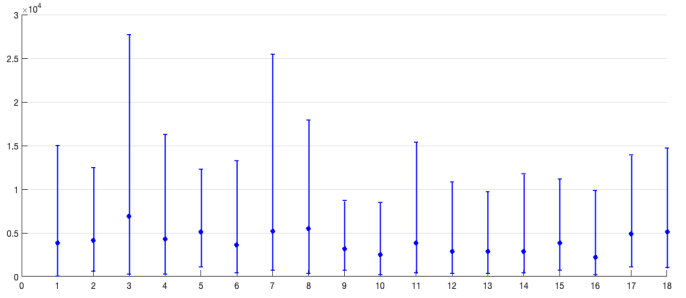Fig. 5. Number n of pointing tasks among all movements and maximum of N_i ($i = 1, \ldots, n$) for users #1 to #18

Fig. 6. The acceleration energy in the x coordinate for users #1 to #18

mouse cursor (0.232418, 18), AVG x-coordinate of mouse cursor (left of page x is 0) (0.214955, 19), AVG velocity of mouse cursor before click (0.208572,21), and other six corresponding to their analogous feature (*e.g.* X coordinates, Maximum).

4. EXPERIMENTAL VALIDATION

Numerous sessions were recorded by each user. In this study, the data from 8 healthy participants (age mean = 48.2, sd = 14.4, 2 female) and 10 PD patients (age mean = 62.8, sd = 12.1, 4 female) were examined. Among the PD patients, 1 was diagnosed less than 5 years ago, 3 between 5 and 10 years ago, 3 between 10 and 15 years ago and 3 between 15 and 20 years ago. In the experiment, a code number is attributed to each user.

To analyze the data, one computer session was chosen arbitrarily for each user. As described in Section 2, the whole dataset was segmented into pointing tasks.

In Fig. 5, the number n of pointing tasks is shown as well the maximum size N_i of the segments for all $i = 1, \ldots, n$, for all users $1, \ldots, 18$ (so the y-axis shows unitless numbers). The numbers in the x-axis are simplified version of the users code numbers and do not correspond the actual codes in the experimental setup. The first 8 users are healthy users (from 1 to 8), while the 10 last are PD patients (from 9 to 18).

All 16 dynamical features presented in Section 3 were computed for each user. To illustrate the obtained results for one of the features, in Fig. 6 it is shown the acceleration energy in the x coordinate, as defined in (3.1). The x-axis represents all 18 users and the y-axis shows the numbers of pixels per ms^2.

The final step was realized via a machine learning toolbox from Matlab. The classification learner toolbox trains several different models to classify a given dataset. This tool allowed the investigation of the proposed features and provided a classification that separated healthy users from PD patients. This is
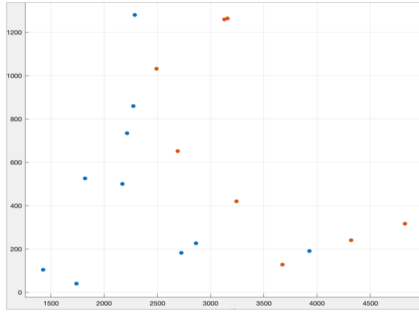
Fig. 7. Scatter plot after training with two features components: *estimation of amplitude of oscillations in y* (max) (3.7) versus the *average of acceleration energy in y* (3.1)

the typical procedure to validate the design of the quantifiers defined in Section 3. All computed features were then utilized to analyze the data. The distinguished classes were determined by the toolbox. At first, all features were used by the learner, used with cross validation. Then a subsequent training with Principal Component Analysis (PCA) followed. As a result, after PCA, two features corresponded to 95% of the variance and according to the Matlab tool, for the classifier Weighted kNN [2] the accuracy is 83.8%. The same accuracy percentage was found by using another method such as the Bagged trees classifier. [3] Note that without cross validation, the accuracy of 100% can be attained.

An example of classifying features is displayed in Fig. 7 with two features components that separate well the two classes: the red dots represent the healthy users and the blue dots indicate PD patients. The axes show the feature *estimation of amplitude of oscillations in y* (max) (3.7) versus the *average of acceleration energy in y* (3.1). The obtained results show that the selected features can be used for discrimination and quantification of tremor presence in controls and Parkison's patients. The used database is sufficient for such a preliminary conclusion, and further the authors will check the approach on a bigger dataset. It is also worth to highlight the existence of many complexities for collecting the data for users.

5. CONCLUSION

To analyze and detect tremor symptoms of PD patients, several dynamical features originating from control theory and applied to a HCI framework were defined in this paper. In particular, a switched model for pointing tasks was utilized, as well as the DREM method to estimate the amplitude of oscillations. All features were defined for a signal produced by a computer mouse providing the position of the cursor on the screen. To validate our results, we used the raw data obtained by a specific non-obstructive experimental setup employed on healthy subjects and PD patients. A classification learning toolkit was deployed resulting in a good accuracy percentage. The proposed method can also be considered as a non-obstructive monitoring of symptoms to optimize treatment for PD patients. In future works, among other possibilities, an extended pointing model involving different transfer functions will be evaluated.

---

[2] Weighted kNN is an altered version of the k nearest neighbors, where a judicious choice of the hyper-parameter k is made.
[3] It consists of an ensemble of decision trees.

REFERENCES

Alves, G., Forsaa, E., Pedersen, K.F., Gjerstad, M., and Larsen, J. (2008). Epidemiology of Parkinson's disease. *Journal of Neurology*, 255, 18–32. doi:10.1007/s00415-008-5004-3.

Aranovskiy, S., Bobtsov, A., Ortega, R., and Pyrkin, A. (2017). Performance enhancement of parameter estimators via dynamic regressor extension and mixing. *IEEE Transactions on Automatic Control*, 62(7), 3546–3550. doi:10.1109/TAC.2016.2614889.

Aranovskiy, S., Ushirobira, R., Efimov, D., and Casiez, G. (2019). A switched dynamic model for pointing tasks with a computer mouse. *Asian Journal of Control*, 0(0).

Casiez, G. and Roussel, N. (2011). No more bricolage!: Methods and tools to characterize, replicate and compare pointing transfer functions. In *Proceedings of the 24th Annual ACM Symposium on User Interface Software and Technology*, UIST '11, 603–614. ACM, New York, NY, USA.

Davidson, C., Paor, A., and Lowery, M. (2012). Insights from control theory into deep brain stimulation for relief from Parkinson's disease. 2–7.

Davie, C.A. (2008). A review of Parkinson's disease. *British medical bulletin*, 86(1), 109–127.

Deuschl, G., Raethjen, J., Lindemann, M., and Krack, P. (2001). The pathophysiology of tremor. *Muscle and Nerve*, 24(6), 716–735.

Dorsey, E., Constantinescu, R., Thompson, J., Biglan, K., Holloway, R., Kieburtz, K., Marshall, F., Ravina, B., Schifitto, G., Siderowf, A., and Tanner, C. (2007). Projected number of people with Parkinson disease in the most populous nations, 2005 through 2030. *Neurology*, 68, 384–6.

Efimov, D. and Fradkov, A. (2015). Design of impulsive adaptive observers for improvement of persistency of excitation. *Int. J. Adaptive Control and Signal Processing*, 29(6), 765–782.

European Parkinson's Disease association (2014). The European Parkinson's disease standards of care consensus statement. Technical report.

Fernandez, L., Huys, R., Issartel, J., Azulay, J.P., and Eusebio, A. (2018). Movement speed-accuracy trade-off in Parkinson's disease. *Frontiers in Neurology*, 9.

García, M.R., Pearlmutter, B.A., Wellstead, P.E., and Middleton, R.H. (2013). A slow axon antidromic blockade hypothesis for tremor reduction via deep brain stimulation. *PLoS ONE*, 8(9), e73456.

Giancardo, L., Sánchez-Ferro, A., Arroyo-Gallego, T., Butterworth, I., Mendoza, C.S., Montero, P., Matarazzo, M., Obeso, J.A., Gray, M.L., and Estépar, R.S.J. (2016). Computer keyboard interaction as an indicator of early Parkinson's disease. *Scientific Reports*, 6, 34468 EP –.

Haddock, A., Velisar, A., Herron, J., Bronte-Stewart, H., and Chizeck, H.J. (2017). Model predictive control of deep brain stimulation for Parkinsonian tremor. In *2017 8th International IEEE/EMBS Conference on Neural Engineering (NER)*, 358–362.

Hartikainen, M. and Ovaska, S. (2015). People with Parkinson's disease using computers. In *Proceedings of the 17th International ACM SIGACCESS Conference on Computers & Accessibility*, ASSETS '15, 407–408. ACM, New York, NY, USA.

Isermann, R. (1997). Supervision, fault-detection and fault-diagnosis methods — an introduction. *Control Engineering Practice*, 5(5), 639 – 652.

Jansson, D., Medvedev, A., Axelson, H., and Nyholm, D. (2015). *Stochastic Anomaly Detection in Eye-Tracking Data for Quantification of Motor Symptoms in Parkinson's Disease*. Springer International Publishing.

Koller, W.C. and Montgomery, E.B. (1997). Issues in the early diagnosis of Parkinson's disease. *Neurology*, 49(1 Suppl 1), S10–S25.

Louis, E.D., Mayer, S.A., and Rowland, L.P. (2015). *Merritt's Neurology*. Lippincott Williams & Wilkins, 13 edition.

Martínez-Martín, P., Gil-Nagel, A., Gracia, L.M., Gómez, J.B., Martínez-Sarriés, J., Bermejo, F., and Group, T.C.M. (1994). Unified Parkinson's disease rating scale characteristics and structure. *Movement Disorders*, 9(1), 76–83.

Medvedev, A., Cubo, R., Olsson, F., Bro, V., and Andersson, H. (2019). Control-engineering perspective on deep brain stimulation: Revisited. In *2019 American Control Conference (ACC)*, 860–865.

Müller, J., Oulasvirta, A., and Murray-Smith, R. (2017). Control theoretic models of pointing. *ACM Trans. Comput.-Hum. Interact.*, 24(4), 27:1–27:36.

Nancel, M., Aranovskiy, S., Ushirobira, R., Efimov, D., Poulmane, S., Roussel, N., and Casiez, G. (2018). Next-Point Prediction for Direct Touch Using Finite-Time Derivative Estimation. In *Proceedings of the ACM Symposium on User Interface Software and Technology (UIST 2018)*. Berlin, Germany.

Olsson, F. and Medvedev, A. (2018). Nonparametric time-domain tremor quantification with smart phone for therapy individualization. *IEEE Transactions on Control Systems Technology*, 1–12.

Oulasvirta, A. (2018). *Computational Interaction*. Oxford University Press.

Pahwa, R., Bergquist, F., Horne, M., and Minshall, M.E. (2020). Objective measurement in Parkinson's disease: a descriptive analysis of Parkinson's symptom scores from a large population of patients across the world using the Personal KinetiGraph®. *Journal of Clinical Movement Disorders*, 7(1), 5.

Pimenta, A., Carneiro, D., Novais, P., and Neves, J. (2013). Monitoring mental fatigue through the analysis of keyboard and mouse interaction patterns. In J.S. Pan, M.M. Polycarpou, M. Woźniak, A.C.P.L.F. de Carvalho, H. Quintián, and E. Corchado (eds.), *Hybrid Artificial Intelligent Systems*, 222–231. Springer Berlin Heidelberg, Berlin, Heidelberg.

Politis, M., Wu, K., Molloy, S., Bain, P., Chaudhuri, K.R., and Piccini, P. (2010). Parkinson's disease symptoms: the patient's perspective. *Mov Disord*, 25(11), 1646–1651.

Sastry, S. and Bodson, M. (1989). *Adaptive Control: Stability, Convergence and Robustness*. Prentice-Hall, London.

Schapira, A.H. and Obeso, J. (2006). Timing of treatment initiation in Parkinson's disease: a need for reappraisal? *Ann Neurol.*, 59(3), 559–562.

Schiff, S.J. (2010). Towards model-based control of Parkinson's disease. *Philosophical transactions. Series A, Mathematical, physical, and engineering sciences*, 368(1918), 2269–2308.

Soukoreff, R.W. and MacKenzie, I.S. (2004). Towards a standard for pointing device evaluation, perspectives on 27 years of Fitts' law research in HCI. *International Journal of Human-Computer Studies*, 61(6), 751 – 789. Fitts' law 50 years later: applications and contributions from human-computer interaction.

Stocchi, F., Vacca, L., and Radicati, F.G. (2015). How to optimize the treatment of early stage Parkinson's disease. *Translational Neurodegeneration*, 4(4).

Wang, J., Efimov, D., Aranovskiy, S., and Bobtsov, A. (2019). Fixed-time estimation of parameters for non-persistent excitation. *European Journal of Control*.

White, R.W., Doraiswamy, P.M., and Horvitz, E. (2018). Detecting neurodegenerative disorders from web search signals. *npj Digital Medicine*, 1(1), 8.